Fluorescent and Electroactive Cyclic Assemblies from Perylene Tetracarboxylic Acid Bisimide Ligands and Metal Phosphane Triflates

Frank Würthner,*[a] Armin Sautter,[a] Dietmar Schmid,[b] and Peter J. A. Weber[c]

Abstract: Tetraaryloxy-substituted perylene tetracarboxylic acid bisimides with one or two 4-pyridyl receptor substituents at the imide functionality were synthesized and employed in transition metal directed self-assembly with Pd^{II} and Pt^{II} phosphane triflates. Upon mixing of the components, quantitative formation of functional molecular square-type complexes containing four dye molecules and model complexes of a 2:1 (perylene bisimide ligand:transition metal ion) stoichiometry was observed. The isolated metallosupramolecular squares were characterized by ^{1}H and ^{31}P $\{^{1}H\}$ NMR spectroscopy as well as conventional electrospray ionization (ESI) and ESI-FTICR mass spectrometry, which gave evidence for the structure and the high stability of these giant cyclic dye assemblies (molecular weight (**3a**) = 8172, Pt–Pt corner diagonal ca. 3.4 nm). Studies of the optical absorption and fluorescence properties and the electrochemistry and spectroelectrochemistry of both the perylene bisimide ligands and the perylene bisimide metal complexes show that Pt^{II} coordination does not interfere with the optical and electrochemical properties of the perylene bisimide ligands; this gives squares with high fluorescence quantum yields (Φ_F (**3a**) = 0.88) and three fully reversible redox couples. The latter could be unambiguously related to quantitative formation of perylene bisimide radical cations ($E_{1/2} = +0.93$ V vs. Fc/Fc^+), radical anions ($E_{1/2} = -1.01$ V vs. Fc/Fc^+), and dianions ($E_{1/2} = -1.14$ V vs. Fc/Fc^+); these redox reactions change the charge state of the cyclic assembly from +12 to zero. In contrast, Pd^{II} coordination influenced the electrochemical properties of the assembly because of an irreversible palladium reduction at $E_{1/2} = -1.15$ V versus Fc/Fc^+. Finally, dynamic ligand exchange processes between different metallosupramolecular assemblies were investigated by multinuclear NMR and electrospray mass spectrometry. These studies confirmed the reversible nature of the pyridine–Pt^{II}/Pd^{II} coordination process.

Keywords: chromophores · cyclic voltammetry · fluorescence · N ligands · supramolecular chemistry

Introduction

The elucidation of the light-harvesting complex of purple bacteria revealed cyclic arrangements of chromophores as a fundamental structural feature for its functionality.[1] Therein, an important aspect is the way that nature assembles a considerable number of chlorophyll and β-carotene dyes by purely noncovalent interactions between the dye molecules and the proteins. This process may be exemplified by Figure 1, where the circles represent the proteins and the rectangles the eight[1c] (or nine)[1a] chlorophyll dyes of the B800 unit (weakly coupled dyes), respectively, in the crystallographically resolved examples (β-carotenes and a second ring of 16 or 18 chlorophyll units (strongly coupled dyes) were omitted for simplicity). Indeed, this kind of structure formation is not only elegant for economic reasons (only one protein has to be encoded at the genetic level for a huge quaternary structure) but results in an assembly of high symmetry that makes all chromophores within the ring structurally and energetically

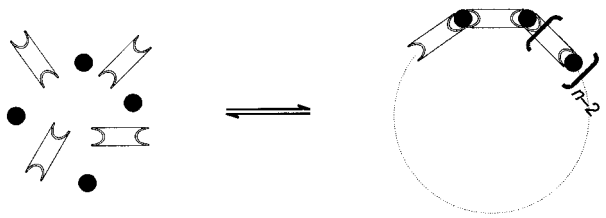

Figure 1. Self-assembly of chromophores to cyclic structures by noncovalent interactions, as in the light-harvesting complex of purple bacteria where $n = 8$[1c] and $n = 9$[1a] are the numbers of chlorophyll units organized in the B800 ring.

[a] Dr. F. Würthner, A. Sautter
Abteilung Organische Chemie II, Universität Ulm
Albert-Einstein-Allee 11, 89081 Ulm (Germany)
Fax: (+49) 731-5022840
E-mail: frank.wuerthner@chemie.uni-ulm.de

[b] D. Schmid
Institut für Organische Chemie, Universität Tübingen
Auf der Morgenstelle 18, 72076 Tübingen (Germany)

[c] Dr. P. J. A. Weber
Fakultät für Biowissenschaften, Pharmazie & Psychologie
Institut für Biochemie, Universität Leipzig
Talstrasse 33, 04103 Leipzig (Germany)

0947-6539/01/0704-0894 $ 17.50+.50/0

equal. This property seems to be important for the energy transfer capabilities of these systems.

Since the discovery of these natural light-harvesting systems, several groups have explored the possibilities for the arrangement of dye molecules in high symmetry in a cyclic fashion by self-assembly.[2–5] The concept of molecular squares introduced by Fujita and Ogura[2a] proved to be especially powerful in the preparation of macrocycles in quantitative yields by a thermodynamically controlled self-assembly process between linear bridging ligands and *cis*-coordinating transition metal ions. Recently, cyclic porphyrin assemblies and luminescent rhenium containing molecular squares were reported,[3c, 4, 5] which show the rapidly increasing interest in the introduction of functional properties in such systems. Indeed, optical and electrochemical addressability in combination with guest inclusion should open up ways toward nanoreactors, in which it might become possible to specifically trigger the reactivity of the enclosed guest molecules.[6] Herein, we present the synthesis and characterization of a new class of molecular squares based on highly fluorescent and electroactive perylene tetracarboxylic acid bisimides that bear 4-pyridine receptor substituents.[7, 8] Coordination of these ligands to *cis*-Pd^{II} and Pt^{II} metal ions results in the formation of cyclic arrangements of four perylene bisimide chromophores in close vicinity in a highly symmetric molecular square-type structure of considerable size in the nanometer regime. For reasons of comparison and simplicity, we also prepared model complexes that contain two monotopic perylene bisimide ligands coordinated to one metal ion corner. We investigated the fluorescence, electrochemical as well as spectroelectrochemical properties of the perylene bisimide ligands and the assemblies containing two and four dyes. Finally, dynamic ligand exchange experiments in mixed systems were evaluated to prove the reversibility of the metal–ligand coordination process, which is of fundamental importance in supramolecular self-organization.

Results and Discussion

Synthesis and characterization of perylene bisimide ligands and perylene bisimide metal complexes: The ditopic perylene bisimide ligands **2** were synthesized by condensation of the corresponding perylene bisanhydrides **1**[8] with 4-aminopyridine in quinoline with catalytic amounts of zinc(II)acetate. The same reaction afforded the monotopic perylene bisimide ligand **6** if a mixture of **1a** and **5**, obtained by partial saponification of the corresponding *N*,*N*′-dibutyl perylene bisimide (see Experimental Section), was allowed to react (Scheme 1). The monotopic ligand **6** could be separated from **2a** by chromatography.

The perylene bisimide metal complexes were prepared in nearly quantitative yields by simply mixing the perylene bisimide ligands with $[M(dppp)][(OTf)_2]$ (dppp = 1,3-bis-(diphenylphosphano)propane; OTf = trifluoromethanesulfonate) in dichloromethane at room temperature (Scheme 1). Precipitation with diethylether afforded analytically pure complexes **3**, **4**, **7**, and **8** that were characterized by elemental analyses, ^1H and $^{31}P\{^1H\}$ NMR spectroscopy, and electrospray mass spectrometry (ESI-MS).

The ^1H NMR spectra of all complexes show species of high symmetry with only a single set of signals for both the dppp moieties and the perylene bisimide ligands and characteristic changes in the chemical shifts for the α- and β-pyridyl protons ($\Delta\delta \approx 0.3$ ppm) with respect to the free ligands (Figure 2a).[9b] All $^{31}P\{^1H\}$ NMR spectra show only one sharp singlet that is shifted upfield by about $\Delta\delta = 10$ ppm with respect to the uncomplexed precursor complexes $[M(dppp)][(OTf)_2]$ ($M = Pt^{2+}/Pd^{2+}$) (Figure 2b).[9b] In addition, ^{195}Pt-^{31}P spin–spin coupling results in Pt satellites in the spectra of **3** and **7**. The α-pyridyl protons and the protons of the dppp ligand exhibit rather broad ^1H NMR signals both in the 2:1 model complexes (**7**, **8**) and the molecular squares (**3a**, **b**, **4**). As no concentration dependence but a distinct temperature dependence could be observed, we attribute this line broadening to conformational flexibility of the dppp unit and not to complex dissociation. A temperature-dependent ^1H NMR study of Pd^{II} complex **8** revealed a coalescence temperature of around 300 K. Below that temperature, each of the broad singlets is split into three signals. At higher temperatures, the broad singlets sharpen notably. Similar observations have already been reported for related metal–dppp–pyridine complexes.[9a, c] The respective X-ray crystal structures revealed that the dppp phenyl rings and the complexing pyridine rings are within the distance of $\pi-\pi$ interaction;[9] thus this restricts the conformational flexibility of the dppp ligand and explains the observed temperature-dependent broad ^1H NMR signals of the α-pyridyl and dppp protons.

ESI-MS allowed us to unambiguously prove the existence of perylene bisimide platinum squares **3a** and **3b**. Additionally, **3a** was investigated by using an Electrospray Fourier Transform Ion Cyclotron mass spectrometer (ESI-FTICR-MS). This technique was used because of both its capability of achieving extremely high mass resolution and the possibility of measuring with a very high mass accuracy.[10] With this method, signals that arise from the isotopic distribution of multiply charged large molecules generated by ESI can be resolved. From the isotopic pattern, the charge state can be derived, and thus the molecular weight can be calculated. In view of the high degree of symmetry of molecule **3a**, it is important to prove that the signal is not caused by a species with a lower charge state but with the same m/z value.

In the overview spectrum (solution of **3a** in acetone), the main signals are the differently charged intact square species $[\mathbf{3a}-3OTf]^{3+}$, $[\mathbf{3a}-4OTf]^{4+}$, $[\mathbf{3a}-5OTf]^{5+}$, and $[\mathbf{3a}-6OTf]^{6+}$ generated by the successive loss of triflate anions (Figure 3). The very high resolution power of FTICR-MS allows unambiguously the assignment of all these signals by way of their characteristic peak separation of 1/3 mass unit for the $[\mathbf{3a}-3OTf]^{3+}$ species, 1/4 mass unit for the $[\mathbf{3a}-4OTf]^{4+}$ species, 1/5 mass unit for the $[\mathbf{3a}-5OTf]^{5+}$ species, and 1/6 mass unit for the $[\mathbf{3a}-6OTf]^{6+}$ species. The experimental masses and isotopic patterns closely match the calculated ones and, with the exception of the signals that are marked with asterisks in Figure 3, all other signals in the spectrum of **3a** could be assigned to fragments of **3a**, for example, loss of one perylene bisimide ligand L ($[\mathbf{3a}-1L]^{n+}$, $n = 2, 3$; m/z 3368.4,

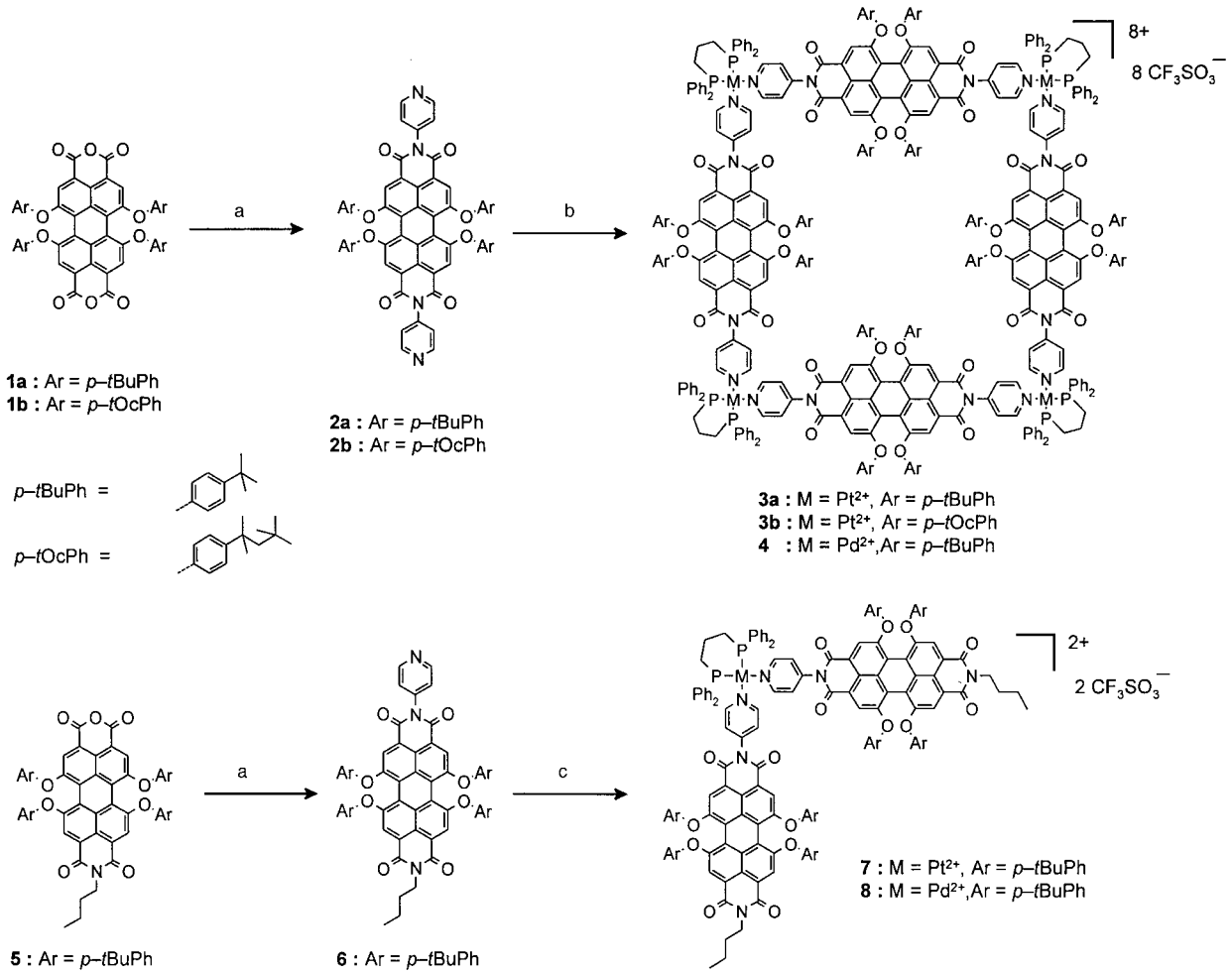

Scheme 1. Synthesis of mono- and ditopic perylene bisimide ligands (**2**, **6**) and formation of perylene bisimide metal squares (**3**, **4**) and model complexes (**7**, **8**): a) 4-aminopyridine, $Zn(OAc)_2$, quinoline, 180 °C, 16 h, argon, 59–66 %; b) [M(dppp)][$(OTf)_2$], CH_2Cl_2, RT, 24 h, argon, 88–94 %; c) [M(dppp)][$(OTf)_2$], CH_2Cl_2, RT, 24 h, argon, 71–89 %.

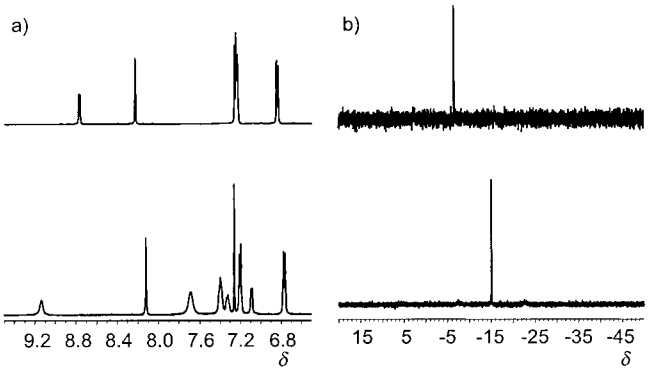

Figure 2. a) ^1H NMR spectra of **2a** (top) and **3a** (bottom); b) ^{31}P {^1H} NMR spectra of [Pt(dppp)][$(OTf)_2$] (top) and **3a** (bottom).

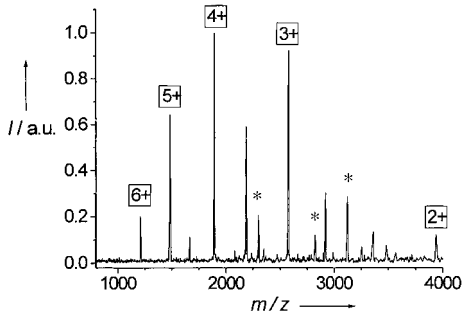

Figure 3. ESI-FTICR-MS of perylene bisimide platinum square **3a** (solution in acetone).

2195.9), loss of one platinum phosphane corner C ($[\mathbf{3a}-1C]^{n+}$, $n=2,4$; m/z 3484.3, 1667.6), and loss of both ($[\mathbf{3a}-1L-1C]^{2+}$, m/z 2915.9).

In Figure 4, the comparison of the measured and calculated spectra of a) the species $[\mathbf{3a}-6OTf]^{6+}$ and b) $[\mathbf{3a}-5OTf]^{5+}$ with a resolution of 60 000 to 50 000 (FWHH, full peak width at half peak height) leaves no doubt about the results. In addition, the 6+ and 5+ charge states of the two species are not multiples of other possible charge states other than 1+ or 3+ and 1+, respectively, so that overlapping with other signals could be excluded. This was confirmed by measuring the species $[\mathbf{3a}-5OTf]^{5+}$ with a resolution of 600 000 (FWHH) in the ultra high resolution mode.

Nonetheless, owing to the less stable Pd–N bond, ESI-MS characterization of the Pd square **4** failed and was difficult for the Pd model complex **8** as thermal and collision dissociation of the Pd complexes predominated in the spectrometer under the applied ESI conditions.

0947-6539/01/0704-0896 $ 17.50+.50/0 *Chem. Eur. J.* **2001**, *7*, No. 4

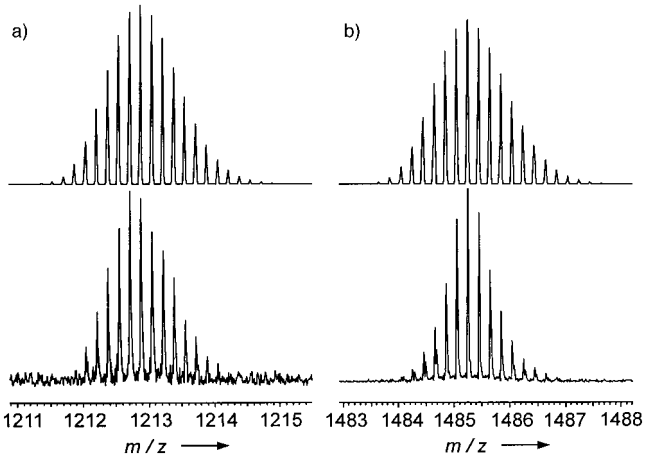

Figure 4. Comparison of the calculated (top) and measured (bottom) spectra a) of the $[\mathbf{3a}-6\mathrm{OTf}]^{6+}$ and b) $[\mathbf{3a}-5\mathrm{OTf}]^{5+}$ species.

Functional properties of perylene bisimide ligands: The optical absorption and fluorescence properties of the ligands **2** and **6** and their relative fluorescence quantum yields Φ_F were investigated. For **2a**, we also studied the electrochemical and spectroelectrochemical properties. All perylene bisimide ligands show an absorption maximum at 585 ± 4 nm and an emission maximum at 618 ± 3 nm in dichloromethane; this shows the negligible effect of the different phenoxy and imide substituents in **2** and **6** on the absorption and emission properties of the tetraphenoxyperylene bisimide chromophore. The UV/Vis and fluorescence spectra of **2a** are shown in Figure 5. The relative fluorescence quantum yields Φ_F are very high and range between 0.88 ± 0.05 (**6**) and 0.94 ± 0.05 (**2a**) in chloroform.

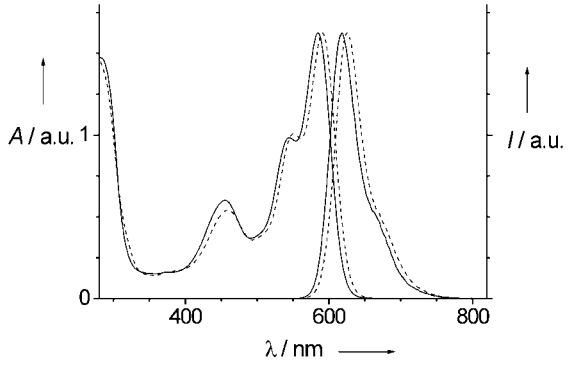

Figure 5. UV/Vis absorption and fluorescence spectra of ditopic perylene bisimide ligand **2a** (——) ($c = 3.5 \times 10^{-5}$ M) and the corresponding perylene bisimide platinum square **3a** (----) ($c = 1.9 \times 10^{-6}$ M) in CH_2Cl_2 ($\lambda_{ex} = 550$ nm).

The electrochemical properties of **2a** were investigated by cyclic voltammetry in dichloromethane (Figure 6). The cyclic voltammogram (CV) of the ditopic perylene bisimide ligand **2a** shows two reversible reductions at $E_{1/2} = -1.08$ V and $E_{1/2} = -1.23$ V, versus ferrocene/ferrocenium (Fc/Fc^+), but the oxidation process is irreversible, and this causes adsorption of **2a** on the platinum electrode. A similar irreversible oxidation process was observed for other azaaromatic conjugated

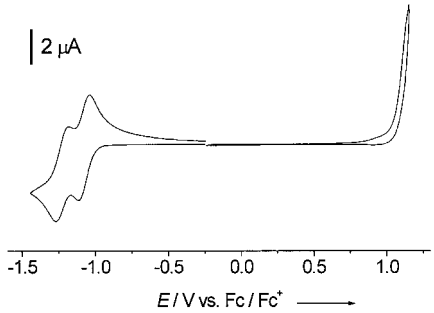

Figure 6. Cyclic voltammogram of ditopic perylene bisimide ligand **2a** in CH_2Cl_2 (sweep rate 100 mV s^{-1}).

systems and attributed to oxidation processes that involve the nitrogen lone pairs.[8d]

To assign the redox couples, **2a** was studied by spectroelectrochemistry, and pronounced changes in the UV/Vis-NIR absorption spectra were observed when a negative potential, that was increased in a stepwise manner, was applied. In the vicinity of the first reduction of **2a**, the absorption bands of the neutral species **2a** diminish (585 nm, 544 nm, 454 nm), while new bands in the NIR appear with a very intense absorption at 792 nm and less intense absorptions at 977 nm and 1085 nm, typical for radical anionic species (Figure 7a). After a further increase of the potential towards the second reduction process, the absorption bands of $\mathbf{2a}^{\bullet-}$ completely disappear, while a broad absorption of tetraphenoxy perylene bisimide dianionic species $\mathbf{2a}^{2-}$ appears at 678 nm (Figure 7b). Thus, **2a** is reduced by two one electron reductions via its radical anionic states $\mathbf{2a}^{\bullet-}$ to the dianionic species $\mathbf{2a}^{2-}$.

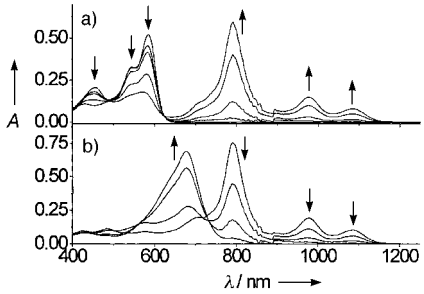

Figure 7. Spectroelectrograms of ditopic perylene bisimide ligand **2a** in CH_2Cl_2. Stepwise increase of the applied potential to a) the first reduction (radical anionic perylene bisimide species $\mathbf{2a}^{\bullet-}$) and b) second reduction of **2a** (dianionic perylene bisimide species $\mathbf{2a}^{2-}$).

Functional properties of perylene bisimide metal complexes: Upon Pd^{II} and Pt^{II} metal coordination, bathochromic shifts of 5–7 nm in the UV/Vis and fluorescence spectra of the perylene bisimide ligands **2** and **6** are observed (Figure 5). For the complexes **3**, **4**, **7**, and **8**, no new optical transitions related to the metal phosphane corners or metal–perylene bisimide charge-transfer bands could be observed in the visible region. As there are no significant changes or new bands in the spectral fine structure, strong excitonic coupling of the complexed perylene bisimide dyes is unlikely.[11] Relative fluorescence quantum yields of $\Phi_F = 0.88 \pm 0.05$ (**3a**) and 0.86 ± 0.05 (**4**) for the perylene bisimide metal squares were determined. In our opinion, this maintenance of

the highly desired fluorescence properties of the perylene bisimide ligands in the metal-coordinated state is due to an electronic decoupling of the coordination sites of the metal-coordinating 4-pyridine unit from the HOMO and LUMO of the perylene bisimide chromophores.[7, 12] As a consequence, the excitation energy is emitted as fluorescence and not quenched by coupling to low-lying MLCT (metal-ligand-charge-transfer) transitions.

The CV of the perylene bisimide platinum square **3a** (Figure 8) exhibits two reversible waves in the reductive cycle ($E_{1/2} = -1.01$ V and $E_{1/2} = -1.14$ V vs. Fc/Fc^+). Upon platinum coordination, both reductions are shifted by about -70 to -90 mV with respect to the perylene bisimide ligand **2a**.

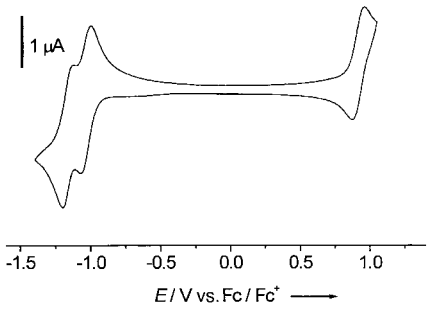

Figure 8. Cyclic voltammogram of perylene bisimide platinum square **3a** in CH_2Cl_2 (sweep rate 100 mV s^{-1}).

Notably, it is possible to reversibly oxidize **3a** at a potential of $E_{1/2} = +0.93$ V, whereas **2a** was irreversibly oxidized and adsorbed onto the platinum electrode. This is probably a consequence of the pyridine platinum coordination, which blocks the nitrogen lone pairs in a sense that they are no longer susceptible to adsorption and facile oxidation. The perylene platinum 2:1 complex **7** shows a similar CV with two reversible reductions ($E_{1/2} = -1.15$ V and $E_{1/2} = -1.29$ V vs. Fc/Fc^+) and one reversible oxidation wave ($E_{1/2} = +0.82$ V). Most interestingly, within the applied potential range, the platinum phosphane corners are not involved in the redox processes.

Further insight into the nature of the redox processes was given by spectroelectrochemical studies of perylene bisimide platinum square **3a**, which could be compared with the experiments of the corresponding perylene bisimide ligand **2a**. An increase in the potential in a stepwise manner towards the first reduction potential of **3a** resulted in a decrease of the UV/Vis absorption bands of **3a**, whereas new transitions in the NIR region appeared with a maximum absorption at 791 nm and weaker transitions at 976 and 1082 nm (Figure 9a). Based on identical changes for the ligand **2a** (Figure 7), these new transitions are unambiguously assigned to perylene bisimide radical anionic species. When the potential is increased to the second reduction potential of **3a**, the UV/Vis-NIR absorption bands of the perylene bisimide radical anionic species completely disappear, while a single broad absorption at 679 nm arises (Figure 9b). Again, the same changes were observed for ligand **2a** (Figure 7) and therefore assigned to the perylene bisimide dianionic species. When a positive potential is applied, new bands appear in the

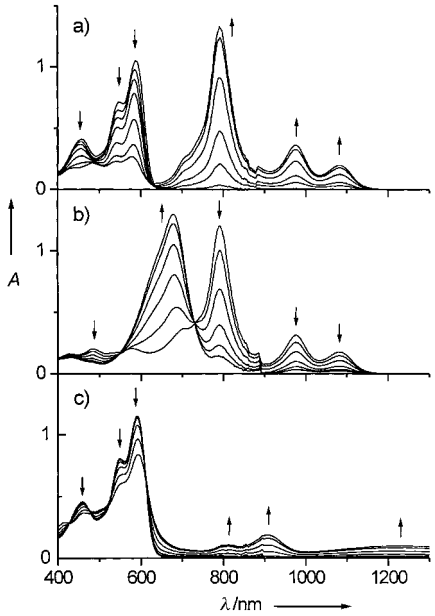

Figure 9. Spectroelectrograms of perylene bisimide platinum square **3a** in CH_2Cl_2. Increase of the applied potential to a) the first reduction, b) second reduction, and c) first oxidation process of **3a**; this generates radical anionic (a), dianionic (b), and radical cationic (c) perylene bisimide species.

NIR at 809 and 908 nm along with a very broad band at 1225 nm (Figure 9c). Although we cannot compare these changes to **2a**, because of its irreversible oxidation, the accompanying changes in the intensities of the perylene bisimide UV/Vis bands let us believe that the perylene bisimide radical cationic species are generated.

Two important conclusions are drawn from these spectroelectrochemical studies: first, we note that the platinum phosphane corner units are electrochemically inert within the applied potential range between -1.3 and $+0.9$ V. They act exclusively as structural building blocks that provide a 90° angle for perylene bisimide ligand coordination. Second, from the complete disappearance of the absorption bands of the neutral and radical anionic species in the spectroelectrochemical experiments we conclude that all four perylene bisimide ligands are independently oxidized and reduced in the square, and this allows us to reversibly switch the charge state of the cyclic perylene bisimide-platinum framework from 0 to $+12$ in steps of four electrons.[13]

The cyclic voltammograms of the palladium complexes **4** and **8** proved to be more complex, since an irreversible palladium reduction is involved. Both the CVs of **4** and **8** display a reversible oxidation at $E_{1/2} = +0.93$ V and $E_{1/2} = +0.84$ V (vs. Fc/Fc^+), respectively, due to the formation of perylene bisimide radical cationic species. The reductions of both complexes show irreversible processes, for example, in the CV of **8** a cathodic peak at -1.15 V appears with no peak in the back scan, followed by the two perylene bisimide reductions (Figure 10). Successive scans resulted in negatively shifted potentials in the respective CVs. We assign the wave at -1.15 V to an irreversible palladium reduction, which might be followed by changes in the coordination geometry of the metal ion. The same occurs in the CV of **4**, but the process is

0947-6539/01/0704-0898 $ 17.50+.50/0 *Chem. Eur. J.* **2001**, *7*, No. 4

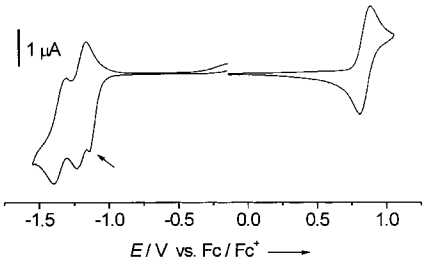

Figure 10. Cyclic voltammogram of perylene bisimide palladium model complex **8** in CH_2Cl_2. The arrow indicates an irreversible palladium reduction.

overlaid by a perylene bisimide reduction in this case, which leads to a significantly more intense first reduction wave. Therefore, the accessible reversible potential range of the perylene bisimide palladium complexes is limited from -1 to about $+1$ V, which only allows us reversibly to switch the charge state of the framework of square **4** between $+8$ and $+12$.

Dynamic ligand exchange processes: The essentially quantitative formation of the molecular square-type complexes is only conceivable by self-assembly with reversible intermolecular coordination interactions. Exchange processes between competing topologies (cyclic vs. linear oligomers) allow self-repairing until the system finally reaches its thermodynamically most stable state under the given experimental conditions. According to a substantial proportion of published work, the rigidity of the building blocks, the linear bridging ligands, the inherent 90° angle of the adjacent coordination sites in the *cis*-protected square planar metal ions, and a low activation energy for the breaking of the metal–pyridine bond are considered to be important factors needed to drive the assembly process to molecular squares to completion. Nevertheless, besides the consistently high yields, little proof of the mechanism of reversible self-assembly is given in the literature of molecular squares so far. If, however, dynamic ligand exchange processes could be observed in solutions of two different squares that result in an equilibrium of different "mixed" square species (as depicted in Figure 11), there are strong arguments for the reversibility of the bond-formation-bond-breaking equilibrium.

Interestingly, such dynamic exchange experiments could rarely be observed for the significant number of squares described in the literature so far. A possible explanation might be the typically different length of the diazaaromatic ligands

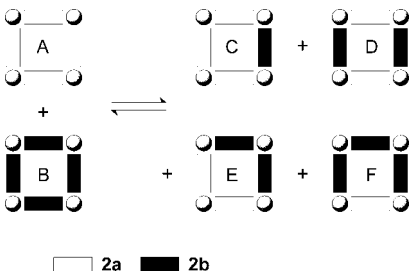

Figure 11. Illustration of a ligand exchange equilibrium in solution after mixing two molecular squares with different ditopic ligands.

that were employed, and this gives preference to the square species containing only ligands of the same type.[9b, 14, 15] Our bridging ligands **2a** and **2b** have the same length and differ only in their alkyl groups at the phenoxy substituents. Accordingly, we considered these ligands well-suited to study exchange processes by ESI-MS and multinuclear NMR spectroscopy.

In a first experiment, we mixed the two perylene bisimide platinum squares **3a** and **3b** in a 1:1 stoichiometry in deuterated chloroform. As shown in Figure 12, the resulting

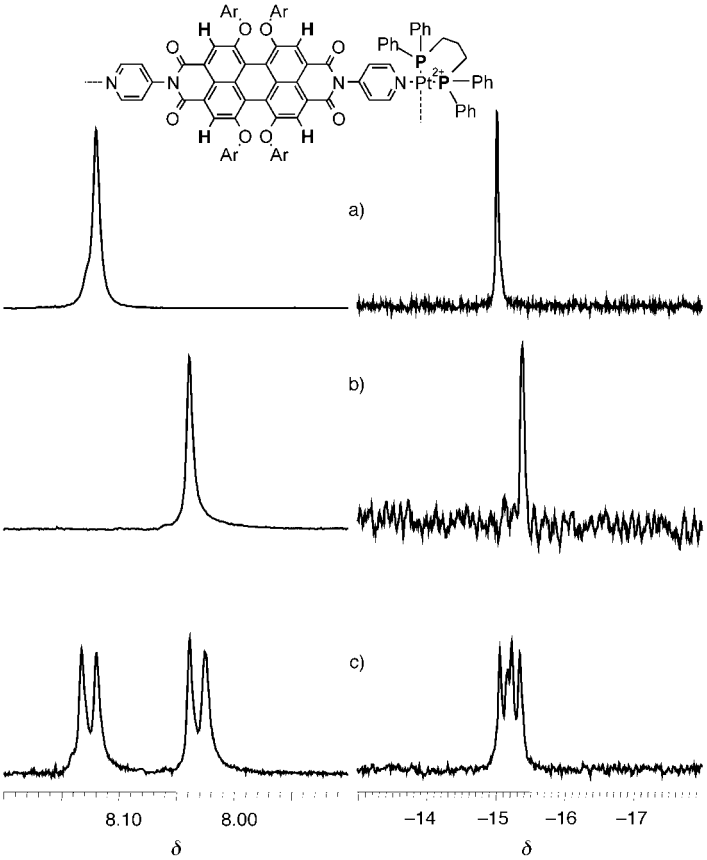

Figure 12. Exchange experiment of perylene bisimide platinum squares **3a** and **3b**. ^{1}H NMR spectra (left) of the perylene bisimide core protons and ^{31}P {^{1}H} NMR spectra (right). Compound **3a** in $CDCl_3$ (a), **3b** in $CDCl_3$ (b), and 1:1 mixture of **3a** and **3b** in $CDCl_3$ (c).

^{1}H and ^{31}P {^{1}H} NMR spectra do not show a simple superposition of the spectra of the two pure squares but reveal a splitting of the signals (no coupling) without line broadening. The fact that sharp signals in the ^{1}H and ^{31}P {^{1}H} NMR spectra still predominate and no endgroups could be detected rules out the formation of long chain oligomeric or polymeric mixtures. Figure 12 shows the signals of the perylene core protons and the ^{31}P {^{1}H} signals of the pure squares **3a** and **3b** and the mixture. If we assume that the limited resolution of the spectrometer allows us only to differentiate between corners with identical ligands and corners with unequal ligands we would expect four singlets for the perylene core protons in the ^{1}H NMR spectrum and four singlets in the ^{31}P {^{1}H} NMR spectrum. For an ideal statistical mixture, we would expect an integral ratio of 1:1 for corners of identical

ligands to corners with unequal ligands for each of the two perylene bisimide ligands.[16] Figure 12 shows that this is exactly the case. We observe an integral ratio of 1:1 and a splitting of each set of perylene core protons and of each set of the phosphane ^{31}P signals into two signals of equal intensity; this gives evidence of the postulated exchange process, which rapidly equilibrated after mixing the two species. Furthermore, the chemical shifts are in accordance with this notion because two of the four signals remain at the positions of the respective pure square species.

In a second experiment, the equilibrium was directly characterized by ESI-MS. The mass spectra were interpreted by the comparison of the experimental masses and charge states with the masses of all possible fragments that might form from the different ligands **2a** and **2b** and the platinum corners. Signals of the intact squares **A**, **B**, and **F** (for assignment of **A**–**F** refer to Figure 11) minus three triflates ($z = 3$) as well as signals of the squares **C** and **D** and/or **E** (we cannot differentiate between **D** and **E** as they exhibit the same masses) minus one platinum corner minus three triflates were detected (Table 1). These signals unambiguously prove the existence of all squares **A**, **B**, **C**, **D**, **E**, and **F** in the equilibrium, exactly as depicted in Figure 11. Smaller fragments with different perylene bisimide ligands could also be detected, but it is not possible to assign them to a distinct species as they could have originated from different squares.

Table 1. Mixed species detected by ESI-MS in the exchange experiment of **3a** and **3b** (dioxane/acetone). The resolution of the spectrometer allowed only the assignment of species with a maximum charge state of $z = 3$. Unresolved signals with a presumably higher charge state were not evaluated.

m/z	z	n(Pt corners)	n(**2a**)	n(**2b**)	m/z (calcd)
2801.1	3	4	1	3	2799.4
2876.9	3	4	0	4	2874.2
2574.9	3	4	4	0	2575.0
2348.1	3	3	3	1	2347.9
2422.7	3	3	2	2	2422.7
2043.9	3	3	1	2	2043.6
2461.9	2	3	1	1	2459.0
2687.5	2	2	1	2	2687.0
2005.0	2	2	1	1	2006.2

Conclusion

The synthesis of ditopic perylene bisimide ligands **2** enabled us to introduce functional properties into Pd and Pt molecular squares **3**. Remarkably, the optical and electrochemical properties of the perylene bisimide ligands are completely conserved in the metal-assembled state. Fluorescence quenching by the metal ions is negligible, and the complexes exhibit multiple reversible redox couples due to the formation of perylene bisimide radical cations, radical anions, and dianions. In the potential range of -1.3 to $+0.95$ V versus Fc/Fc^+, the Pt^{II}–phosphane corners act purely as structural building blocks that allow undisturbed switching of the perylene bisimide ligands' redox states. However, the reversible potential range of the Pd square is limited to -1.1 V versus Fc/Fc^+ when Pd^{II} undergoes an irreversible reduction process. Furthermore, we showed that dynamic ligand exchange processes take place in solution at room temperature to yield defined mixed molecular squares containing statistical amounts of ligands **2a** and **2b**.

Experimental Section

Materials and methods: Solvents and reagents were purchased from Merck unless otherwise stated and purified and dried according to standard procedures.[17] *N,N′*-Dibutyl-1,6,7,12-tetra(4-*tert*-butylphenoxy)perylene-3,4:9,10-tetracarboxylic acid bisimide, 1,6,7,12-tetra(4-*tert*-butylphenoxy)-perylene-3,4:9,10-tetracarboxylic acid bisanhydride **1a**, 1,6,7,12-tetra(4-(1,1,3,3-tetramethylbutyl)phenoxy)perylene-3,4:9,10-tetracarboxylic acid bisanhydride **1b**,[8] [Pd(dppp)][$(OTf)_2$]·$2H_2O$ (dppp = 1,3-bis-(diphenylphosphano)propane; OTf = trifluoromethanesulfonate),[9b] and [Pt(dppp)]-[$(OTf)_2$]·$2H_2O$[9b] were synthesized according to the literature. Column chromatography was performed on silica gel (Merck Silica 60, particle size 0.063–0.2 mm). UV/Vis spectra were recorded on a Perkin-Elmer Lambda 40P spectrometer, and fluorescence spectra were recorded on a Perkin-Elmer LS 50B fluorometer. Fluorescence quantum yields were determined relative to *N,N′*-di(2,6-diisopropylphenyl)-1,6,7,12-tetraphenoxyperylene-3,4:9,10-tetracarboxylic acid bisimide ($\Phi_R = 0.96$, $CHCl_3$)[8a, 8e] by the optically dilute method[18] ($A \leq 0.04$) in chloroform. NMR spectra were recorded on a Bruker DRX 400 and a Bruker AMX 500 spectrometer with TMS as internal standard. Electrospray mass spectra were taken on a Perkin-Elmer Sciex single quadrupol API 100 spectrometer. ESI-FTICR-MS measurements were carried out with a passively shielded 4.7 Tesla APEXII-ESI-FT-ICR mass spectrometer from Bruker Daltonik (Bremen, Germany). A saturated solution of **3a** in acetone was used. For mass calculation, data acquisition, processing, and apodization, the mass spectrometry software XMASS version 5.0.7 (Bruker Daltonik) was used. The number of data points was 512 K for acquisition and 1M for processing within a mass range of 500–4000 Da. To increase the signal-to-noise ratio, 100 scans were accumulated. For the external four-point calibration, an ES Tuning Mix from Hewlett Packard (Waldbronn, Germany) was used. The calculated m/z values corresponded to the average masses, and the experimental (found) m/z values corresponded to the respective peak with the highest intensity.

Electrochemistry: Cyclic voltammetry was performed with an EG&G PAR 273 potentiostat in a three-electrode single compartment cell with dichloromethane as solvent (5 mL). Working electrode: platinum disk; counterelectrode: platinum wire; reference electrode: Ag/AgCl. All potentials were internally referenced to the Fc/Fc^+ couple. The solutions were purged with argon prior to use. The supporting electrolyte was 0.1M [Bu_4N][PF_6] (Fluka), which was recrystallized twice from ethanol/water and dried in a high vacuum. The experimental setup for spectroelectrochemistry has been described by Salbeck.[19]

Exchange experiments: For NMR experiments, solutions of the squares **3a** and **3b** were prepared in $CDCl_3$ at a concentration of 5 mM. The solutions were mixed 1:1 by volume and kept overnight at room temperature before the measurement.

For ESI-MS studies, solutions of approximately the same concentration of the squares **3a** and **3b** were prepared in dioxane and mixed 1:1 by volume. The resulting solution was diluted with acetone (1:1 by volume) and stored at room temperature overnight in a sealed vial. ESI mass spectra were recorded from this solution.

N,N′-Di(4-pyridyl)-1,6,7,12-tetra(4-tert-butylphenoxy)perylene-3,4:9,10-tetracarboxylic acid bisimide (***2a***): 1,6,7,12-Tetra(4-*tert*-butylphenoxy)perylene-3,4:9,10-tetracarboxylic acid bisanhydride **1a** (296 mg, 0.3 mmol), 4-aminopyridine (Fluka, 94 mg, 1.0 mmol), and zinc(II)acetate (Fluka, 30 mg, 0.16 mmol) were stirred under argon at 180 °C for 16 h in quinoline (10 mL). HCl (2N, 50 mL) was added, and the precipitate was collected, washed with water and methanol, and dried. Column chromatography (CH_2Cl_2/MeOH 98:2) afforded **2a** (225 mg, 66%). M.p. > 300 °C; ^1H NMR (500 MHz, $CDCl_3$, 25 °C, TMS): $\delta = 8.77$ (d, $^3J(H,H) = 5.6$ Hz, 4H; $H_{\alpha\text{-py}}$), 8.23 (s, 4H), 7.24 (m, 12H; H_{ar}+$H_{\beta\text{-py}}$), 6.84 (d, $^3J(H,H) = 8.7$ Hz, 8H; H_{ar}), 1.27 (s, 36H; H_{tBu}); UV/Vis (CH_2Cl_2): λ_{max} (ε) = 585 (46100), 545 (28000), 455 (17000), 268 nm (44900 $mol^{-1}dm^3cm^{-1}$); fluorescence (CH_2Cl_2):

0947-6539/01/0704-0900 $ 17.50+.50/0 *Chem. Eur. J.* **2001**, *7*, No. 4

$\lambda_{max} = 618$ nm; fluorescence quantum yield ($CHCl_3$): $\Phi_F = 0.94$; FAB-MS (*m*-NBA, *m*-nitrobenzyl alcohol): *m/z* (%): calcd 1137.3; found 1137.6; elemental analysis calcd (%) for $C_{74}H_{64}N_4O_8$ (1137.3): C 78.15, H 5.67, N 4.93; found C 77.90, H 5.68, N 4.94.

N,N′-Di(4-pyridyl)-1,6,7,12-tetra(4-(1,1,3,3-tetramethylbutyl)phenoxy)perylene-3,4:9,10-tetracarboxylic acid bisimide (**2b**): The compound 1,6,7,12-tetra(4-(1,1,3,3-tetramethylbutyl)phenoxy)perylene-3,4:9,10-tetracarboxylic acid bisanhydride **1b** (363 mg, 0.3 mmol), 4-aminopyridine (94 mg, 1.0 mmol), and zinc(II)acetate (30 mg, 0.16 mmol) were allowed to react and worked up in the same way as described for **2a** to give **2b** (240 mg, 59%). M.p. > 300 °C; ^{1}H NMR (400 MHz, $CDCl_3$, 25 °C, TMS): $\delta = 8.77$ (d, $^3J(H,H) = 6.2$ Hz, 4H; $H_{\alpha\text{-py}}$), 8.17 (s, 4H), 7.28 (d, $^3J(H,H) = 8.7$ Hz, 8H; H_{ar}), 7.23 (d, $^3J(H,H) = 6.2$ Hz, 4H; $H_{\beta\text{-py}}$), 6.88 (d, $^3J(H,H) = 8.7$ Hz, 8H; H_{ar}), 1.71 (s, 8H; H_{CH2}), 1.34 (s, 24H; H_{CH3}), 0.75 (s, 36H; H_{tBu}); UV/Vis (CH_2Cl_2): λ_{max} (ε) = 588 (48800), 547 (28800), 454 (17700), 268 nm (46200 $mol^{-1} dm^3 cm^{-1}$); fluorescence (CH_2Cl_2): $\lambda_{max} = 621$ nm; MALDI-TOF-MS (dithranol): *m/z* (%): calcd 1361.8; found 1362.7; elemental analysis calcd (%) for $C_{90}H_{96}N_4O_8$ (1361.8): C 79.38, H 7.11, N 4.11; found C 79.16, H 7.10, N 3.97.

N-(4-Pyridyl)-N′-butyl-1,6,7,12-tetra(4-tert-butylphenoxy)perylene-3,4:9,10-tetracarboxylic acid bisimide (**6**): Partial saponification of *N,N′*-dibutyl-1,6,7,12-tetra(4-*tert*-butylphenoxy)perylene-3,4:9,10-tetracarboxylic acid bisimide (7.67 g, 7 mmol) with KOH (150 g, 267 mmol) in isopropyl alcohol (1000 mL) and H_2O (100 mL) under argon by stirring at reflux for 15 h, followed by acidic workup, and thorough washing and drying, yielded a mixture (5.8 g) of perylene bisanhydride **1a** and perylene mono butylimide monoanhydride **5** in a ratio of about 6:4. This mixture (1.48 g) was reacted in the same way as described for **2a** with 4-aminopyridine (0.47 g, 5.0 mmol) and zinc(II)acetate (0.18 g, 0.8 mmol) in quinoline (30 mL) at 180 °C for 16 h. After workup and chromatography on a Merck-Lobar-C (LiChroprep Si60) column (CH_2Cl_2/MeOH 98:2), **2a** (0.52 g) and **6** (0.38 g) were isolated. Compound **6**: m.p. > 300 °C; ^{1}H NMR (500 MHz, $CDCl_3$, 25 °C, TMS): $\delta = 8.77$ (d, $^3J(H,H) = 5.9$ Hz, 2H; $H_{\alpha\text{-py}}$), 8.24 (s, 2H), 8.23 (s, 2H), 7.26–7.21 (m, 10H; H_{ar}+$H_{\beta\text{-py}}$), 6.84 (m, 8H; H_{ar}), 4.12 (t, 2H), 1.66 (m, 2H), 1.39 (m, 2H), 1.29 (s, 18H; H_{tBu}), 1.27 (s, 18H; H_{tBu}), 0.94 (t, 3H); UV/Vis (CH_2Cl_2): λ_{max} (ε) = 581 (45200), 542 (27800), 453 (17200), 286 nm (45200 $mol^{-1} dm^3 cm^{-1}$); fluorescence (CH_2Cl_2): $\lambda_{max} = 615$ nm; fluorescence quantum yield ($CHCl_3$): $\Phi_F = 0.88$; MALDI-TOF-MS (dithranol): *m/z* (%): calcd 1116.4; found 1116.4; elemental analysis calcd (%) for $C_{73}H_{69}N_3O_8$ (1116.4): C 78.54, H 6.23, N 3.76; found C 78.32, H 6.25, N 3.43.

Perylene bisimide platinum square (**3a**): [Pt(dppp)][$(OTf)_2$]·2H_2O (141.3 mg, 0.15 mmol) and ditopic perylene **2a** (170.6 mg, 0.15 mmol) were stirred under argon at room temperature for 24 h in CH_2Cl_2 (30 mL). After filtration, the solution was concentrated to 5 mL, and diethylether was added to precipitate **3a**. The solid was collected by centrifugation, washed twice with diethylether (5 mL), and dried in vacuo at 50 °C to afford a violet solid (274 mg, 88%). M.p. > 300 °C; ^{1}H NMR (500 MHz, $CDCl_3$, 25 °C, TMS): $\delta = 9.13$ (brs, 16H; $H_{\alpha\text{-py}}$), 8.12 (s, 16H), 7.69 (brs, 32H; $H_{ar(dppp)}$), 7.40 (m, 32H; $H_{ar(dppp)}$), 7.32 (m, 16H; $H_{ar(dppp)}$), 7.20 (d, $^3J(H,H) = 8.4$ Hz, 32H; H_{ar}), 7.09 (d, $^3J(H,H) = 5.9$ Hz, 16H; $H_{\beta\text{-py}}$), 6.77 (d, $^3J(H,H) = 8.4$ Hz, 32H; H_{ar}), 3.29 (brs, 16H; H_{P-CH2}), 2.20 (brs, 8H; H_{CH2}), 1.24 (s, 144H; H_{tBu}); ^{31}P {^{1}H} NMR (202 MHz, $CDCl_3$, 25 °C, 85% H_3PO_4): $\delta = -15.11$ (s); UV/Vis (CH_2Cl_2): λ_{max} (ε) = 591 (217000), 550 (135000), 459 nm (72000 $mol^{-1} dm^3 cm^{-1}$); fluorescence (CH_2Cl_2): $\lambda_{max} = 625$ nm; fluorescence quantum yield ($CHCl_3$): $\Phi_F = 0.88$; ESI-FTICR-MS (acetone): *m/z* (%): calcd for $[M - 2OTf]^{2+}$: 3936.969; found 3936.906; calcd for $[M - 3OTf]^{3+}$: 2574.957; found 2574.779; calcd for $[M - 4OTf]^{4+}$: 1893.950; found 1894.056; calcd for $[M - 5OTf]^{5+}$: 1485.346; found 1485.256; calcd for $[M - 6OTf]^{6+}$: 1212.944; found 1212.716; elemental analysis calcd (%) for $C_{412}H_{360}N_{16}O_{56}F_{24}P_8Pt_4S_8 \cdot 8H_2O$ (8316.4): C 59.50, H 4.56, N 2.69, S 3.08; found C 59.29, H 4.59, N 2.54, S 3.03.

Perylene bisimide platinum square (**3b**): [Pt(dppp)][$(OTf)_2$]·2H_2O (47.1 mg, 0.05 mmol) and ditopic perylene **2b** (68.1 mg, 0.05 mmol) were allowed to react and worked up in the same way as described for **3a** to give a violet solid (104 mg, 91%). M.p. > 300 °C; ^{1}H NMR (500 MHz, $CDCl_3$, 25 °C, TMS): $\delta = 9.13$ (brs, 16H; $H_{\alpha\text{-py}}$), 8.04 (s, 16H), 7.67 (brs, 32H; $H_{ar(dppp)}$), 7.39 (m, 32H; $H_{ar(dppp)}$), 7.31 (m, 16H; $H_{ar(dppp)}$), 7.25 (d, $^3J(H,H) = 8.4$ Hz, 32H; H_{ar}), 7.07 (brs, 16H; $H_{\beta\text{-py}}$), 6.82 (d, $^3J(H,H) = 8.4$ Hz, 32H; H_{ar}), 3.28 (brs, 16H; H_{P-CH2}), 2.20 (brs, 8H; H_{CH2}), 1.68 (s, 32H; H_{CH2}), 1.32 (s, 96H; H_{CH3}), 0.70 (s, 144H; H_{tBu}); ^{31}P {^{1}H} NMR (202 MHz, $CDCl_3$, 25 °C, 85% H_3PO_4): $\delta = -15.47$ (s); UV/Vis (CH_2Cl_2): λ_{max} (ε) = 592 (214400), 551 (131700), 458 nm (71000 $mol^{-1} dm^3 cm^{-1}$); fluorescence (CH_2Cl_2): $\lambda_{max} = 628$ nm; ESI-MS (acetone): *m/z* (%): calcd for $[M - 3OTf]^{3+}$: 2874.2; found 2874.5; elemental analysis calcd (%) for $C_{476}H_{488}N_{16}O_{56}F_{24}P_8Pt_4S_8 \cdot 4H_2O$ (9141.8): C 62.54, H 5.47, N 2.45, S 2.81; found C 62.57, H 5.42, N 2.33, S 2.74.

Perylene bisimide palladium square (**4**): [Pd(dppp)][$(OTf)_2$]·2H_2O (128.0 mg, 0.15 mmol) and ditopic perylene **2a** (170.6 mg, 0.15 mmol) were allowed to react and worked up in the same way as described for **3a** to give a violet solid (280 mg, 94%). M.p. 304 °C (decomp); ^{1}H NMR (500 MHz, $CDCl_3$, 25 °C, TMS): $\delta = 9.09$ (brs, 16H; $H_{\alpha\text{-py}}$), 8.12 (s, 16H), 7.66 (m, 32H; $H_{ar(dppp)}$), 7.40–7.30 (m, 48H; $H_{ar(dppp)}$), 7.20 (d, $^3J(H,H) = 8.7$ Hz, 32H; H_{ar}), 7.04 (d, $^3J(H,H) = 5.6$ Hz, 16H; $H_{\beta\text{-py}}$), 6.77 (d, $^3J(H,H) = 8.7$ Hz, 32H; H_{ar}), 3.20 (brs, 16H; H_{P-CH2}), 2.23 (brs, 8H; H_{CH2}), 1.24 (s, 144H; H_{tBu}); ^{31}P {^{1}H} NMR (202 MHz, $CDCl_3$, 25 °C, 85% H_3PO_4): $\delta = 6.66$ (s); UV/Vis (CH_2Cl_2): λ_{max} (ε) = 590 (218000), 549 (136000), 458 nm (74000 $mol^{-1} dm^3 cm^{-1}$); fluorescence (CH_2Cl_2): $\lambda_{max} = 624$ nm; fluorescence quantum yield ($CHCl_3$): $\Phi_F = 0.86$; elemental analysis calcd (%) for $C_{412}H_{360}N_{16}O_{56}F_{24}P_8Pd_4S_8 \cdot 8H_2O$ (7961.4): C 62.16, H 4.76, N 2.81, S 3.22; found C 62.37, H 4.61, N 2.81, S 3.29.

Perylene bisimide platinum (*2:1-complex* **7**): [Pt(dppp)][$(OTf)_2$]·2H_2O (38.0 mg, 0.041 mmol) and monotopic perylene **6** (89.3 mg, 0.08 mmol) were allowed to react in CH_2Cl_2 (20 mL) and worked up as described for **3a** to give a violet solid (90 mg, 71%); M.p. > 300 °C; ^{1}H NMR (500 MHz, $CDCl_3$, 25 °C, TMS): $\delta = 9.14$ (brs, 4H; $H_{\alpha\text{-py}}$), 8.20 (s, 4H), 8.15 (s, 4H), 7.69 (brs, 8H; $H_{ar(dppp)}$), 7.38 (brs, 8H; $H_{ar(dppp)}$), 7.34 (brs, 8H; $H_{ar(dppp)}$), 7.25–7.19 (m, 16H; H_{ar}), 7.11 (brs, 16H; $H_{\beta\text{-py}}$), 6.82–6.79 (m, 16H; H_{ar}), 4.11 (t, 4H; H_{Bu}), 3.29 (brs, 4H; H_{P-CH2}), 2.20 (brs, 2H; H_{CH2}), 1.65 (m, 4H; H_{Bu}), 1.39 (m, 4H; H_{Bu}), 1.29 (s, 36H; H_{tBu}), 1.24 (s, 36H; H_{tBu}), 0.93 (t, 6H; H_{Bu}); ^{31}P {^{1}H} NMR (202 MHz, $CDCl_3$, 25 °C, 85% H_3PO_4): $\delta = -15.14$ (s); UV/Vis (CH_2Cl_2): λ_{max} (ε) = 586 (99000), 547 (61000), 455 (35000), 285 nm (98000 $mol^{-1} dm^3 cm^{-1}$); fluorescence (CH_2Cl_2): $\lambda_{max} = 619$ nm; ESI-MS (acetone): *m/z* (%): calcd for $[M - 2OTf]^{2+}$: 1420.1; found 1420.0; elemental analysis calcd (%) for $C_{175}H_{164}N_6O_{22}F_6P_2PtS_2 \cdot 2H_2O$ (3174.4): C 66.21, H 5.33, N 2.65, S 2.02; found C 66.32, H 5.36, N 2.60, S 2.07.

Perylene bisimide palladium (*2:1-complex* **8**): [Pd(dppp)][$(OTf)_2$]·2H_2O (16.3 mg, 0.02 mmol) and monotopic perylene **6** (42.5 mg, 0.038 mmol) in CH_2Cl_2 (5 mL) were allowed to react and worked up as described for **3a** to yield of violet solid (52 mg, 89%); M.p. 285 °C (decomp); ^{1}H NMR (500 MHz, $CDCl_3$, 25 °C, TMS): $\delta = 9.10$ (brs, 4H; $H_{\alpha\text{-py}}$), 8.20 (s, 4H), 8.15 (s, 4H), 7.65 (brs, 8H; $H_{ar(dppp)}$), 7.39–7.35 (m, 12H; $H_{ar(dppp)}$), 7.21 (m, 16H; H_{ar}), 7.05 (brs, 4H; $H_{\beta\text{-py}}$), 6.80 (m, 16H; H_{ar}), 4.11 (t, 4H; H_{Bu}), 3.20 (brs, 4H; H_{P-CH2}), 2.22 (brs, 2H; H_{CH2}), 1.65 (m, 4H; H_{Bu}), 1.39 (m, 4H; H_{Bu}), 1.29 (s, 36H; H_{tBu}), 1.24 (s, 36H; H_{tBu}), 0.93 (t, 6H; H_{Bu}); ^{31}P {^{1}H} NMR (202 MHz, $CDCl_3$, 25 °C, 85% H_3PO_4): $\delta = 6.61$ (s); UV/Vis (CH_2Cl_2): λ_{max} (ε) = 584 (99000), 545 (61000), 455 (35000), 283 (98000), 267 nm (122000 $mol^{-1} dm^3 cm^{-1}$); fluorescence (CH_2Cl_2): $\lambda_{max} = 618$ nm; ESI-MS (acetone): *m/z* (%): calcd for $(M - 2OTf)^{2+}$: 1376.8; found 1375.7; elemental analysis calcd (%) for $C_{175}H_{164}N_6O_{22}F_6P_2PdS_2 \cdot 2H_2O$ (3085.8): C 68.12, H 5.49, N 2.72, S 2.08; found C 68.31, H 5.45, N 2.71, S 2.10.

Acknowledgements

This work was supported by Fonds der Chemischen Industrie and BMBF (Liebig grant for F.W.), DFG (Habilitation grant for F.W.), and the Ulmer Universitätsgesellschaft (startup grant). We gratefully acknowledge BASF AG and Degussa-Hüls AG for the donation of chemicals and Prof. P. Bäuerle (Ulm) and Prof. G. Jung (Tübingen) for helpful discussions.

[1] a) G. McDermott, S. M. Prince, A. A. Freer, A. M. Hawthornthwaite-Lawless, M. Z. Papiz, R. J. Cogdell, N. W. Isaacs, *Nature* **1995**, *374*, 517–521; b) T. Pullerits, V. Sundström, *Acc. Chem. Res.* **1996**, *29*, 381–389; c) X. Hu, K. Schulten, *Phys. Today* **1997**, *50(8)*, 28–38.

[2] a) M. Fujita, J. Yazaki, K. Ogura, *J. Am. Chem. Soc.* **1990**, *112*, 5645–5647; b) M. Fujita, K. Ogura, *Bull. Chem. Soc. Jpn.* **1996**, *69*, 1471–1482; c) M. Fujita, *Acc. Chem. Res.* **1999**, *32*, 53–61.

[3] a) S. Leininger, B. Olenyuk, P. J. Stang, *Chem. Rev.* **2000**, *100*, 853–908; b) J. Manna, C. J. Kuehl, J. A. Whiteford, P. J. Stang, D. C. Muddiman, S. A. Hofstadler, R. D. Smith, *J. Am. Chem. Soc.* **1997**, *119*,

11611 – 11619; c) J. Fan, J. A. Whiteford, B. Olenyuk, M. D. Levin, P. J. Stang, E. B. Fleischer, *J. Am. Chem. Soc.* **1999**, *121*, 2741 – 2752.
[4] a) R. V. Slone, D. I. Yoon, R. M. Calhoun, J. T. Hupp, *J. Am. Chem. Soc.* **1995**, *117*, 11813 – 11814; b) R. V. Slone, K. D. Benkstein, S. Belanger, J. T. Hupp, *Coord. Chem. Rev.* **1998**, *171*, 221 – 243; c) R. V. Slone, J. T. Hupp, *Inorg. Chem.* **1997**, *36*, 5422 – 5423; d) S.-S. Sun, A. J. Lees, *Inorg. Chem.* **1999**, *38*, 4181 – 4182; e) S. M. Woessner, J. B. Helms, Y. Shen, B. P. Sullivan, *Inorg. Chem.* **1998**, *37*, 5406 – 5407; f) S. M. Woessner, J. B. Helms, J. F. Houlis, B. P. Sullivan, *Inorg. Chem.* **1999**, *38*, 4380 – 4381.
[5] a) C. M. Drain, J. M. Lehn, *J. Chem. Soc. Chem. Commun.* **1994**, 2313 – 2315; b) C. M. Drain, F. Nifiatis, A. Vasenko, J. D. Batteas, *Angew. Chem.* **1998**, *110*, 2478 – 2481; *Angew. Chem. Int. Ed.* **1998**, *37*, 2344 – 2347; c) K. Funatsu, T. Imamura, A. Ichimura, Y. Sasaki, *Inorg. Chem.* **1998**, *37*, 1798 – 1804.
[6] a) D. J. Cram, M. E. Tanner, R. Thomas, *Angew. Chem.* **1991**, *103*, 1048 – 1051; *Angew. Chem. Int. Ed. Engl.* **1991**, *30*, 1024 – 1027; b) R. Warmuth, *Angew. Chem.* **1997**, *109*, 1406 – 1409; *Angew. Chem. Int. Ed. Engl.* **1997**, *36*, 1345 – 1350; c) J. Kang, J. Rebek, Jr., *Nature* **1997**, *385*, 50 – 52.
[7] A part of this work appeared in a short communication: F. Würthner, A. Sautter, *Chem. Commun.* **2000**, 445 – 446.
[8] a) G. Seybold, G. Wagenblast, *Dyes Pigm.* **1989**, *11*, 303 – 317; b) D. Dotcheva, M. Klapper, K. Müllen, *Macromol. Chem. Phys.* **1994**, *195*, 1905 – 1911; c) F. Würthner, C. Thalacker, A. Sautter, *Adv. Mater.* **1999**, *11*, 754 – 758; d) F. Würthner, C. Thalacker, A. Sautter, *Angew. Chem.* **2000**, *112*, 1298 – 1301; *Angew. Chem. Int. Ed.* **2000**, *39*, 1243 – 1245; e) R. Gvishi, R. Reisfeld, Z. Burshtein, *Chem. Phys. Lett.* **1993**, *213*, 338 – 344.
[9] a) M. Fuss, H. U. Siehl, B. Olenyuk, P. J. Stang, *Organometallics* **1999**, *18*, 758 – 769; b) P. J. Stang, D. H. Cao, S. Saito, A. M. Arif, *J. Am. Chem. Soc.* **1995**, *117*, 6273 – 6283; c) E. Iengo, B. Milani, E. Zangrando, S. Geremia, E. Alessio, *Angew. Chem.* **2000**, *112*, 1138 – 1141; *Angew. Chem. Int. Ed.* **2000**, *39*, 1096 – 1099.
[10] a) A. G. Marshall, C. L. Hendrickson, G. S. Jackson, *Mass Spectrom. Rev.* **1998**, *17*, 1 – 35; b) I. J. Amster, *J. Mass Spectrom.* **1996**, *31*, 1325 – 1337.
[11] Molecular modeling suggests that opposite perylene bisimide dyes in the molecular squares have a distance of about 2.4 nm. The energy-minimized structure is boxlike. However, ^{1}H NMR spectroscopy indicates that in solution the rotation of the perylene bisimide chromophores around the imide–pyridyl N–C bond is a fast process and that there is no preferred orientation of the perylene bisimide chromophores towards each other. If this rotation was hindered it should be possible to distinguish between the inner and outer region of the molecular square by ^{1}H NMR spectroscopy which is not the case.
[12] It is well established that the HOMO and LUMO of perylene bisimides exhibit nodes at the imide nitrogens: a) S. K. Lee, Y. Zu, A. Herrmann, Y. Geerts, K. Müllen, A. J. Bard, *J. Am. Chem. Soc.* **1999**, *121*, 3513 – 3520; b) H. Langhals, S. Demmig, H. Huber, *Spectrochim. Acta Part A* **1988**, *44*, 1189 – 1193.
[13] Attempts to determine the number of electrons involved in the redox processes of **3a** by comparison with a known quantity of ferrocene or by bulk electrolysis were not successful. This is probably due to the large differences in diffusion coefficients. In addition, **3a** might not be sufficiently stable under the applied conditions of bulk electrolysis.
[14] K. D. Benkstein, J. T. Hupp, C. L. Stern, *J. Am. Chem. Soc.* **1998**, *120*, 12982 – 12983.
[15] An interesting experiment has been reported by Stang and co-workers on an assembly process that involves *trans*-Pt–phosphane species and results in the formation of a statistical mixture of molecular squares: J. Manna, C. J. Kuehl, J. A. Whiteford, P. J. Stang, D. C. Muddiman, S. A. Hofstadler, R. D. Smith, *J. Am. Chem. Soc.* **1997**, *119*, 11611 – 11619.
[16] The expected probabilities for the squares in the equilibrium are **A** (6.25%), **B** (6.25%), **C** (25%), **D** (12.5%), **E** (25%), and **F** (25%) if a completely independent incorporation of the ligands **2a** and **2b** is assumed.
[17] D. D. Perrin, W. L. F. Armarego, *Purification of Laboratory Chemicals*, 2nd ed., Pergamon, Oxford, **1980**.
[18] J. N. Demas, G. A. Crosby, *J. Phys. Chem.* **1971**, *75*, 991 – 1024.
[19] J. Salbeck, *J. Electroanal. Chem.* **1992**, *340*, 169.

Received: June 29, 2000 [F2576]

0947-6539/01/0704-0902 $ 17.50+.50/0